

Supporting Information for

Statistical Downscaling of Coastal Directional Wave Spectra Using Deep Learning

Tianxiang Gao ¹, Haoyu Jiang ^{*1, 2, 3}

1 Hubei Key Laboratory of Marine Geological Resources, China University of Geosciences, Wuhan, China

2 Laboratory for Regional Oceanography and Numerical Modeling, Qingdao National Laboratory for Marine Science and Technology, Qingdao, China

3 Shenzhen Research Institute, China University of Geosciences, Shenzhen, China

Contents of this file

Figures S1 to S15

Introduction

The supporting information shows the results of all downscaling experiments for all five buoy locations used in this study. It contains the following information:

1. Figures S1-S5: The comparison of directional wave spectra (DWSs) between the results from dynamic downscaling and those from Deep Learning (DL) downscaling with different input parameters.
2. Figure S6-S10: The comparison of Integral Wave Parameters (IWPs) between the results from dynamic downscaling and those from DL downscaling with different input parameters, as well as between those from buoy observations and those from DL downscaling.
3. Figure S11-S15: The comparison of DWSs between the results from buoy reconstruction and from DL downscaling using buoy data as training targets.

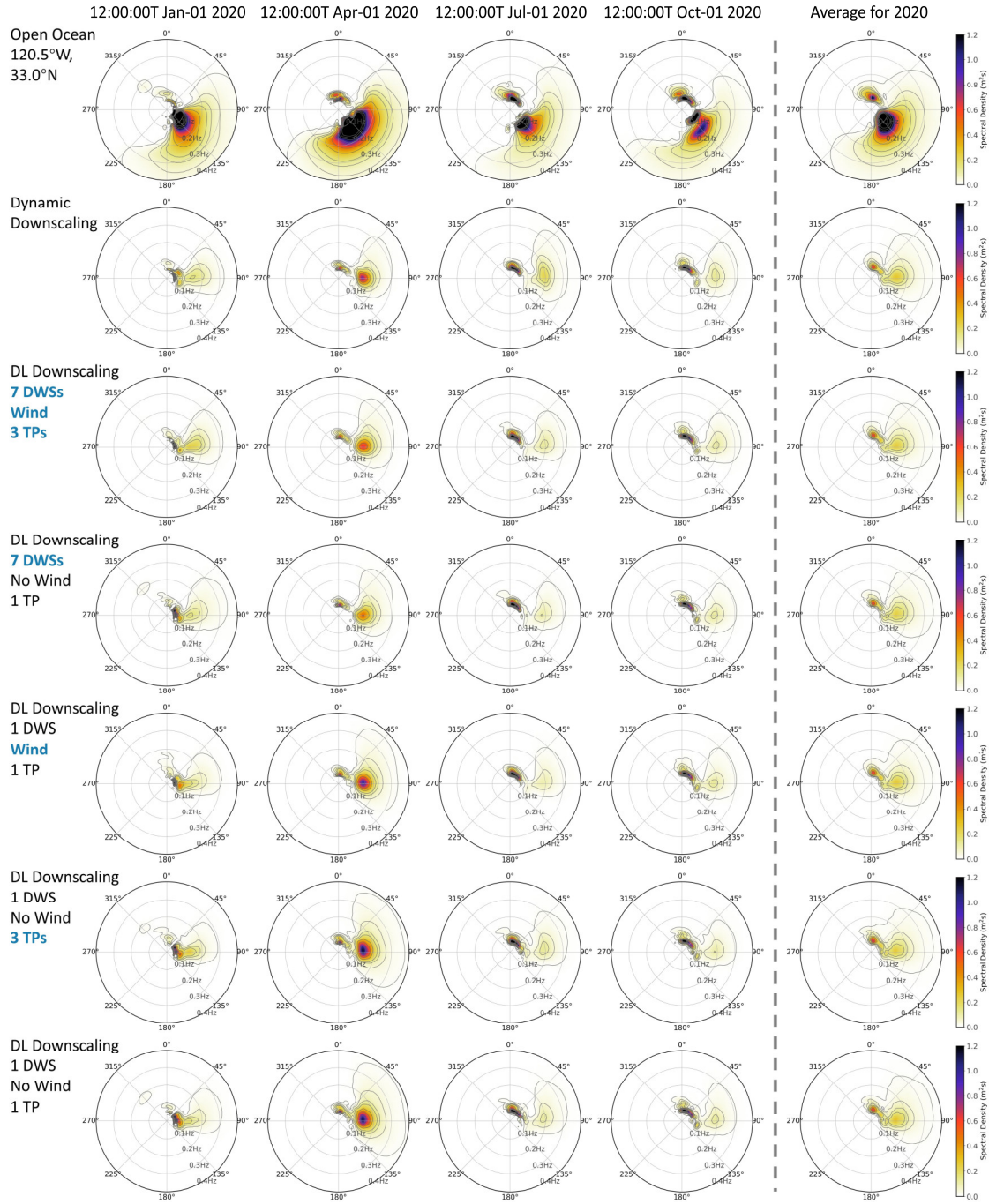


Figure S1. The comparison of directional wave spectra (DWSs) between the results from dynamic downscaling and those from Deep Learning (DL) downscaling with different input parameters at the location of buoy CDIP028. The 1st row is the DWSs at the open boundary point (120.5°W, 33.0°N) before downscaling. The 2nd row shows the corresponding dynamic-downscaled DWSs from IOWAGA at the buoy location. The 3rd-7th rows show the results from the DL downscaling model using IOWAGA DWSs as the training target, but with different input parameters. The input parameters for the 3rd row include open boundary DWSs at seven locations and at three time points, and the wind vector at the buoy location (the results shown in Figure 2 in the main text). Those for the 4th row include open boundary DWSs at seven locations but only at one time point, without the

wind vector input. Those for the 5th row include the open boundary DWS at only one location and at only one time point, but with the wind vector input. Those for the 6th row include the open boundary DWSs at only one location but at three time points, without the wind vector input. Those for the 7th row include only the open boundary DWS at only one location and at only one time point, without the wind vector input. The four columns to the left of the dashed line in each row are the corresponding DWSs at four arbitrarily selected time points. The seven DWSs to the right of the dashed line in each row are the corresponding annual mean DWSs in 2020.

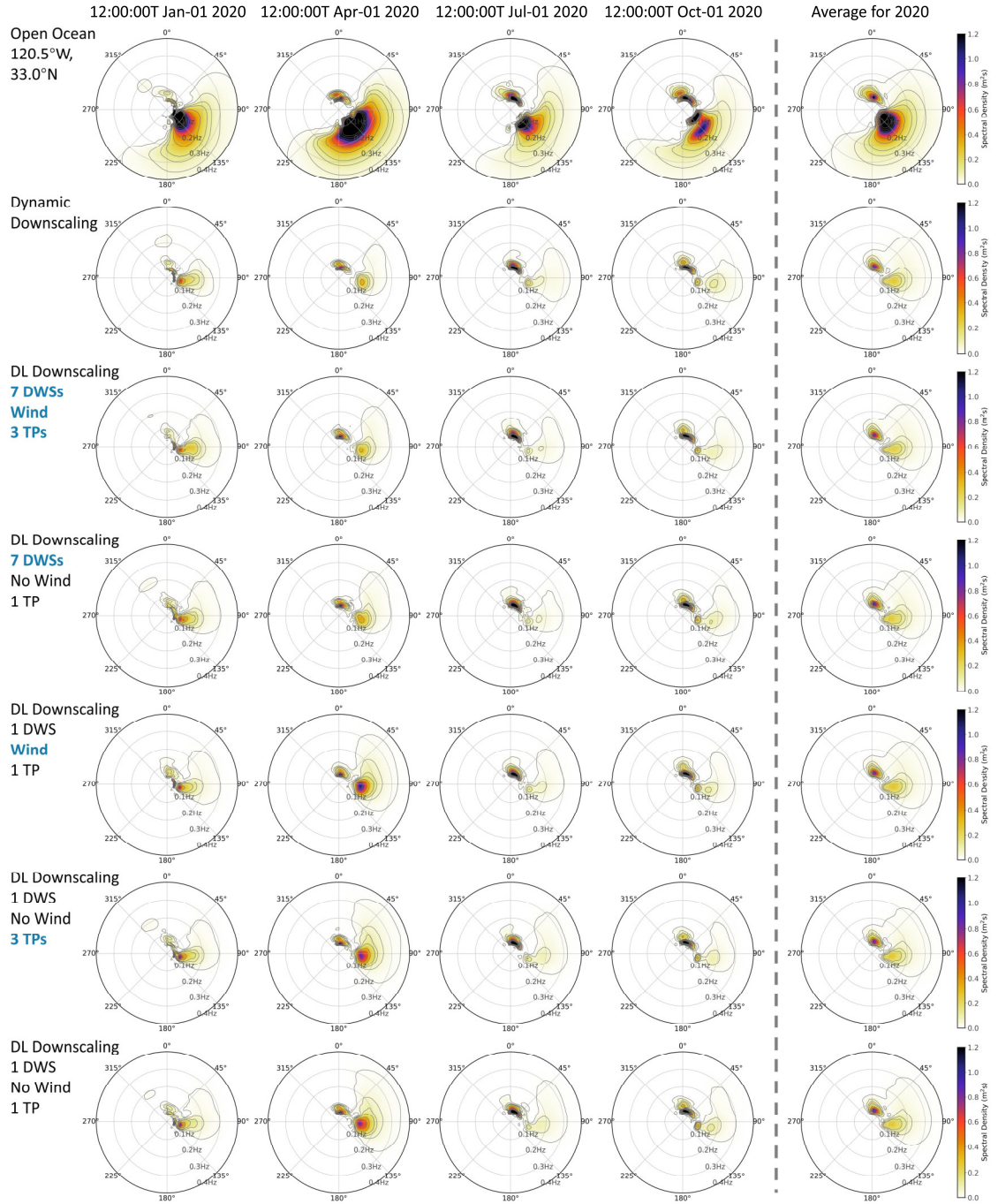


Figure S2. The same as Figure S1, but for buoy CDIP045.

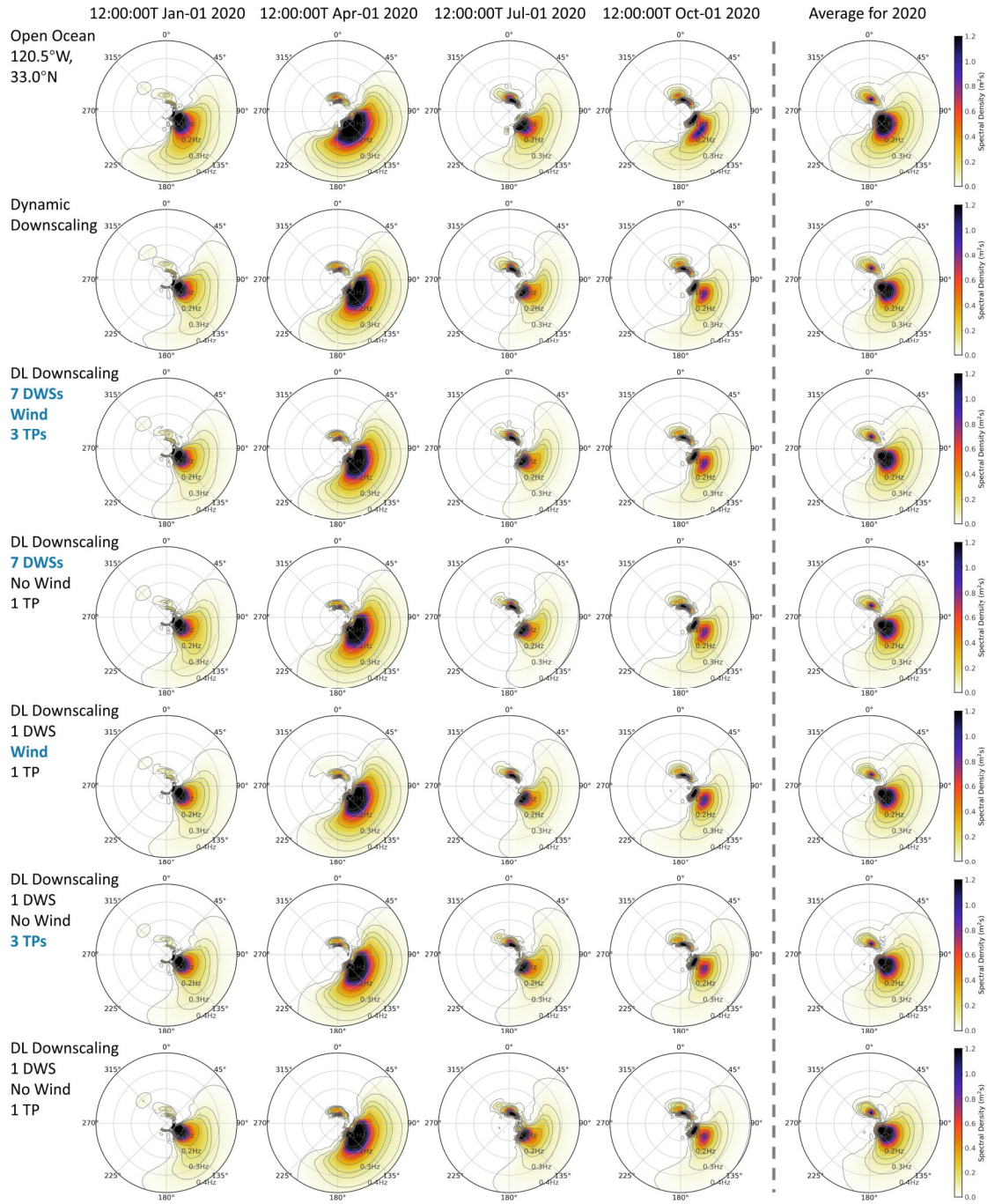


Figure S3. The same as Figure S1, but for buoy CDIP067.

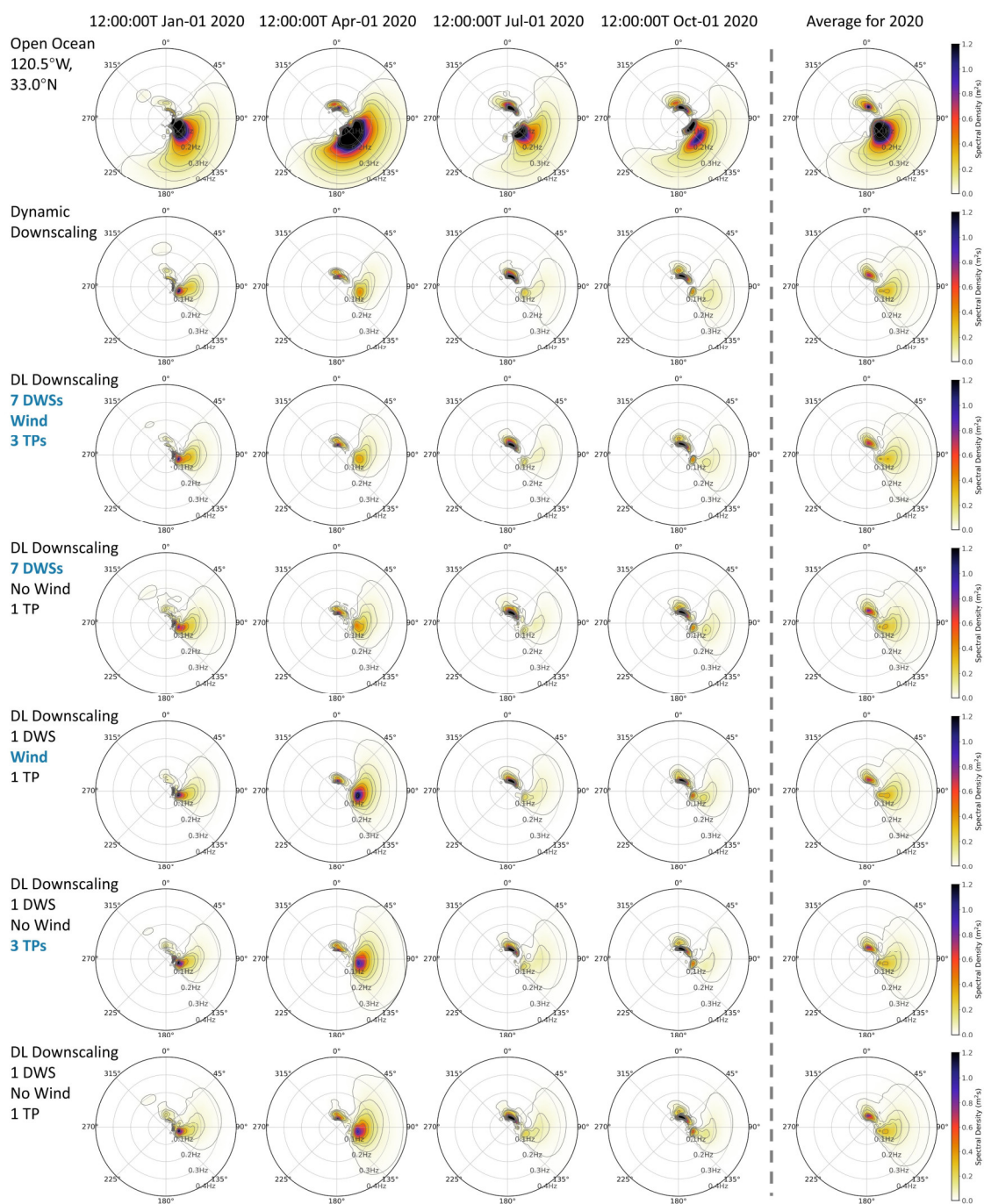


Figure S4. The same as Figure S1, but for buoy CDIP093.

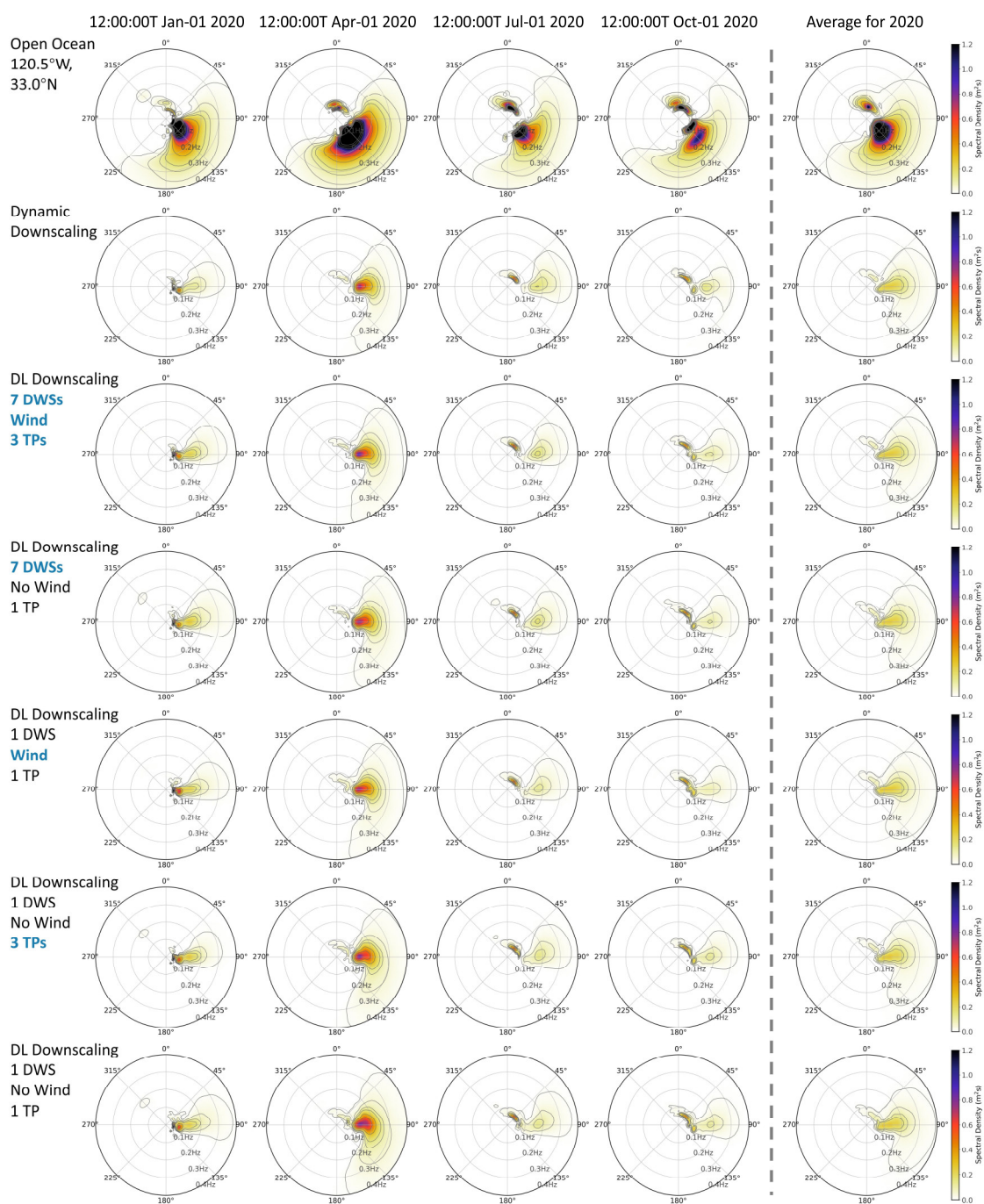


Figure S5. The same as Figure S1, but for buoy CDIP107.

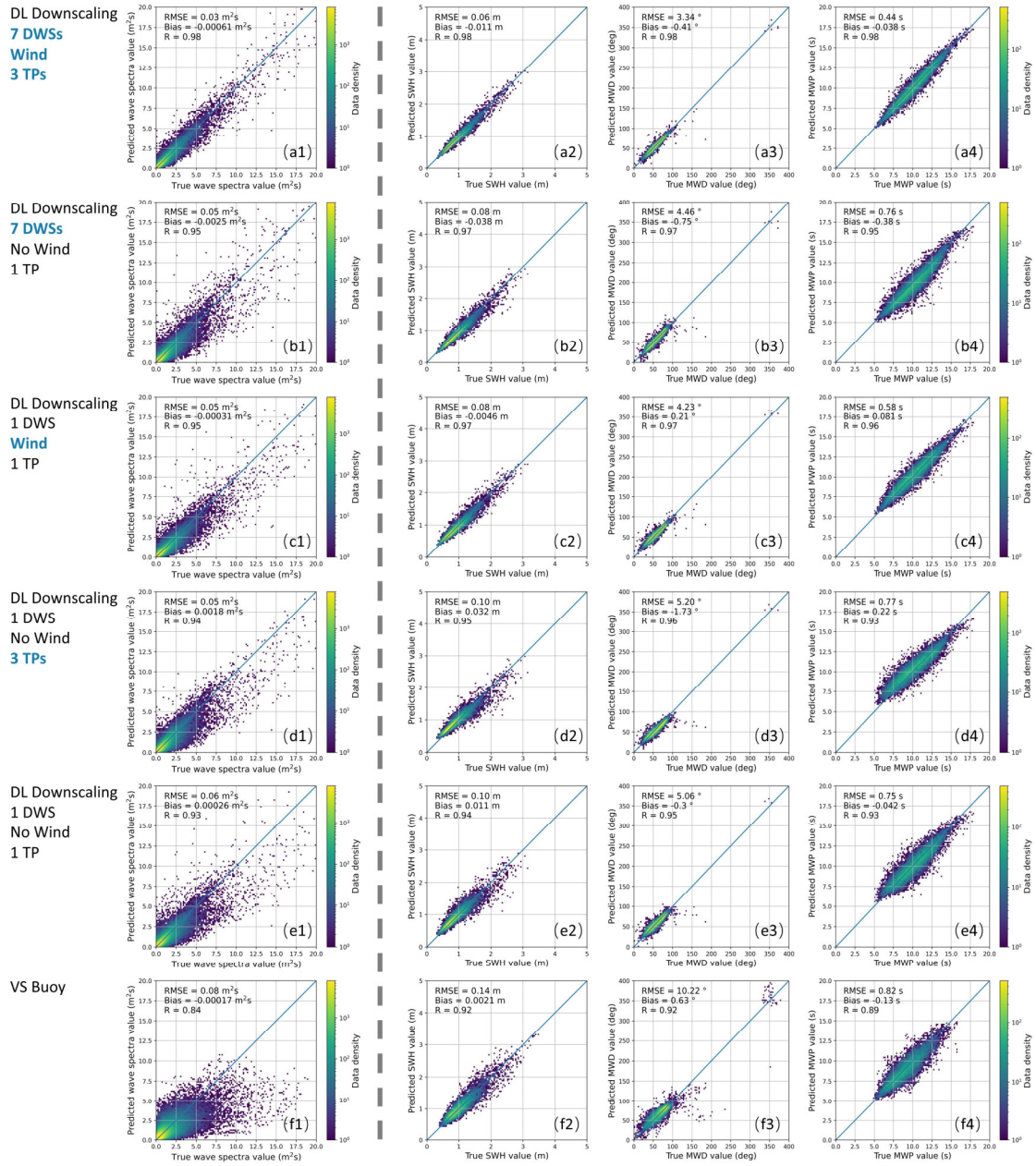


Figure S6. Scatter plots between Deep Learning (DL) downscaling results and their corresponding reference data with different input parameters and training targets at the location of buoy CDIP028. The 1st-5th rows show the comparison between the DL-downscaled results using IOWAGA directional wave spectra (DWSs) as training targets and the dynamic-downscaled results, but with different input parameters. The input parameters for the 1st row include open boundary DWSs at seven locations and at three time points, and the wind vector at the buoy location (the results shown in Figures 3a-3d in the main text). Those for the 2nd row include open boundary DWSs at seven locations but only at one time point, without the wind vector input. Those for the 3rd row include the open boundary DWS at only one location and at only one time point, but with the wind vector input. Those for the 4th row include the open boundary DWSs at only one location but at three time points, without the wind vector input. Those for the 5th row include only the open boundary DWS at only one location and at only one time point, without the wind vector input. The 6th row is the

comparison between DL-downscaled results (using buoy DWS as training targets) and buoy data (the results shown in Figures 3e-3h in the main text). The four columns are the comparison for (the 1st column) spectral densities, (the 2nd column) SWH, (the 3rd column) MWD, and (the 4th column) MWP, respectively.

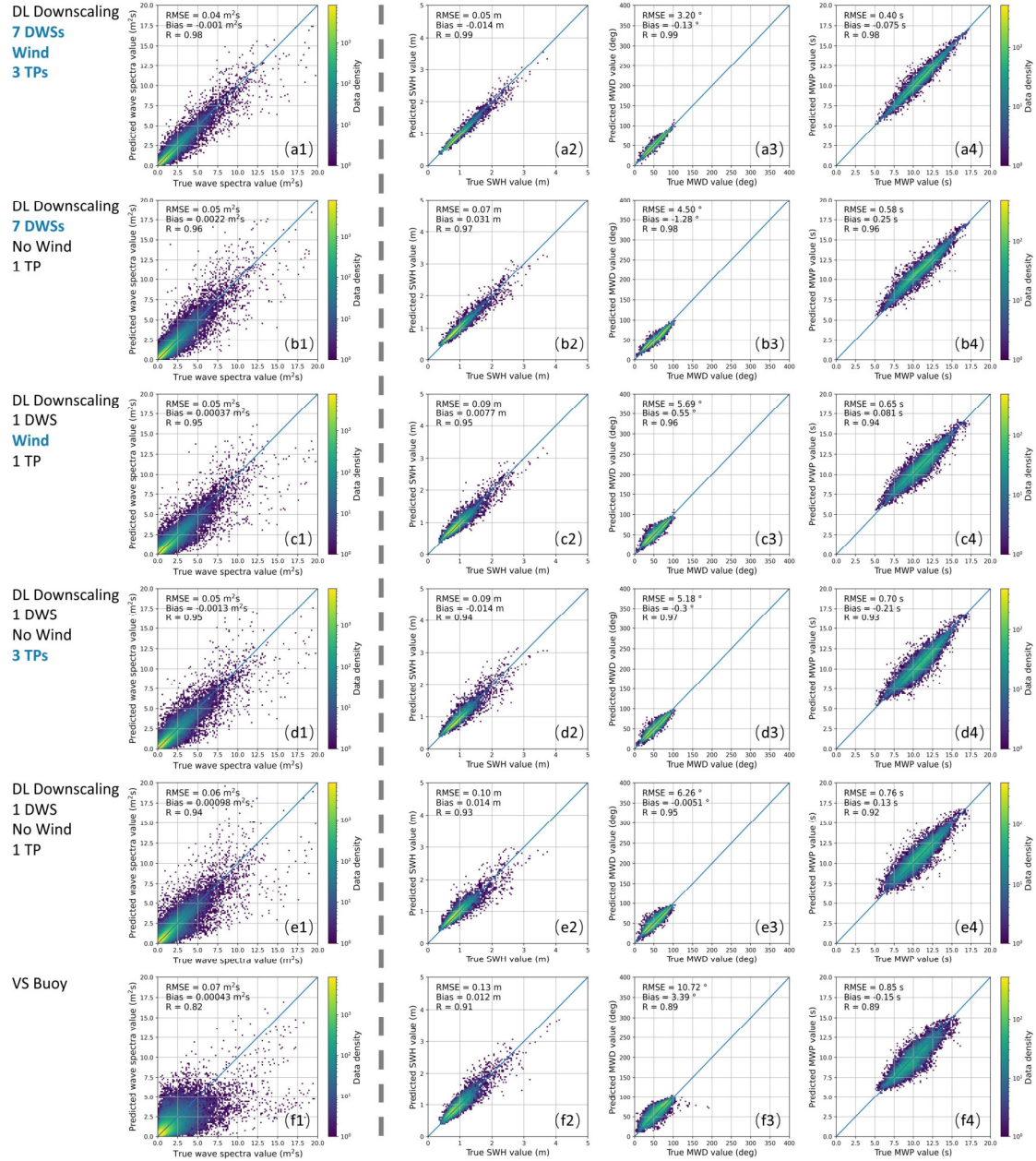


Figure S7. The same as Figure S6, but for buoy CDIP045.

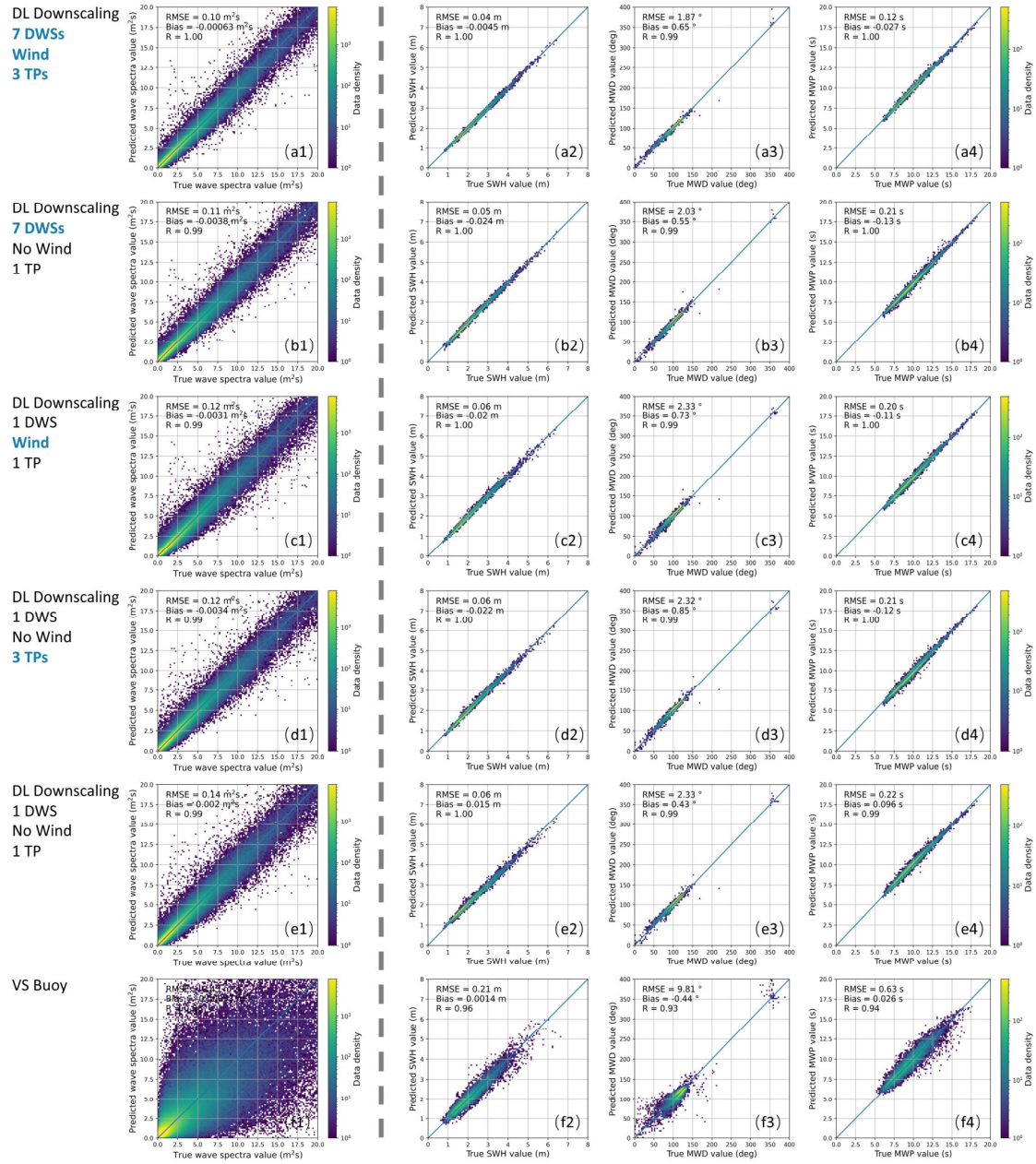


Figure S8. The same as Figure S6, but for buoy CDIP067.

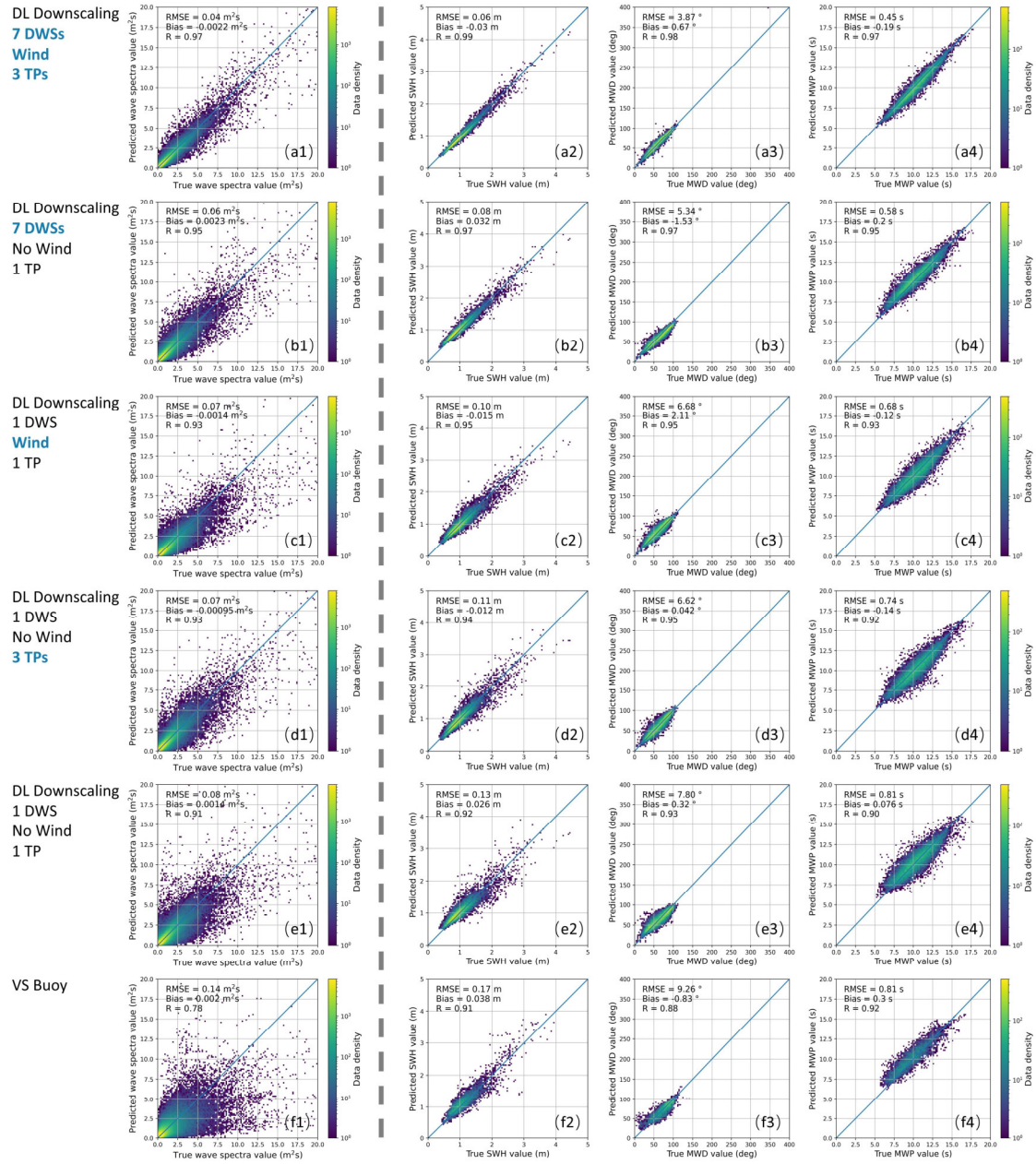


Figure S9. The same as Figure S6, but for buoy CDIP093.

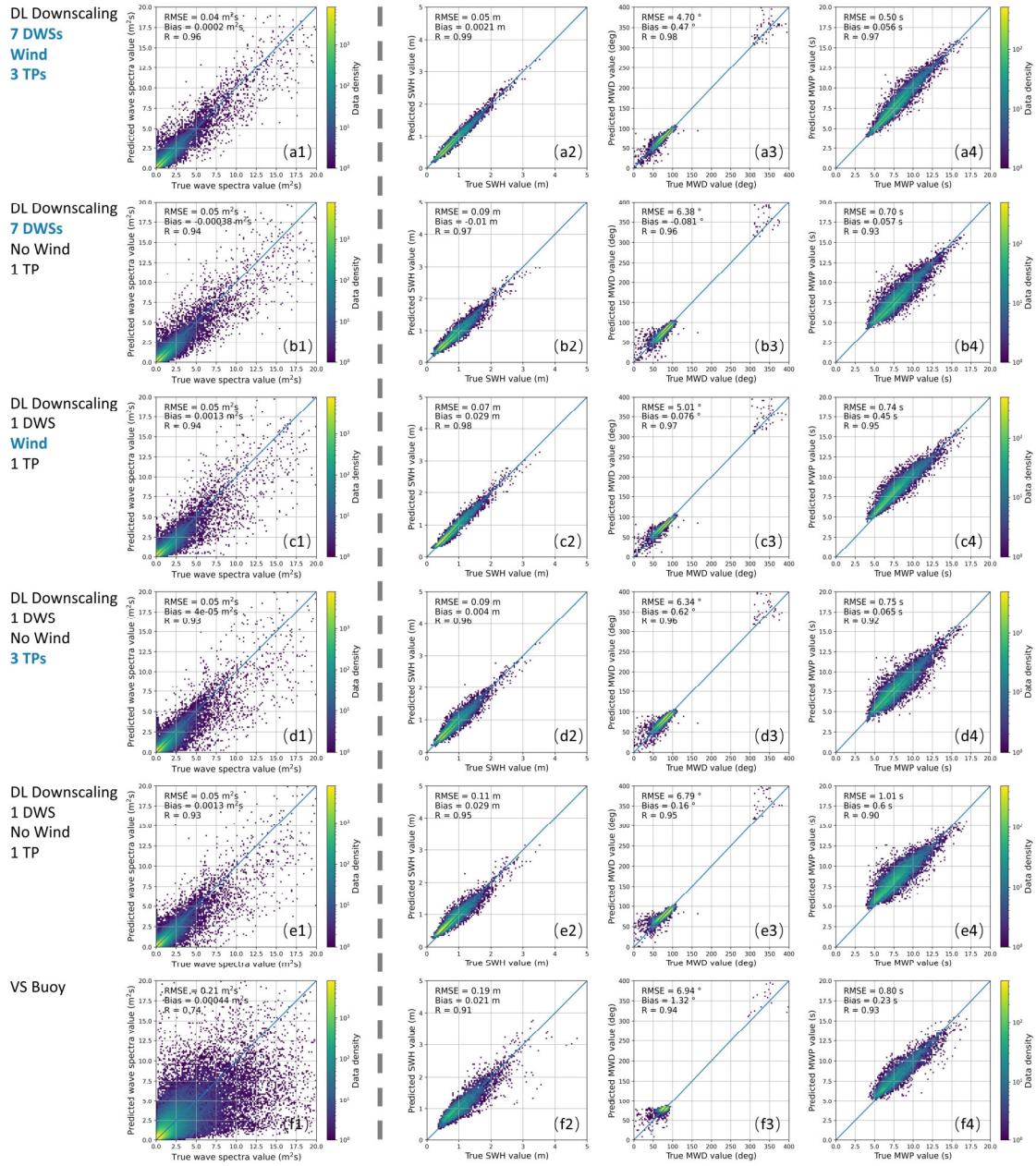


Figure S10. The same as Figure S6, but for buoy CDIP107.

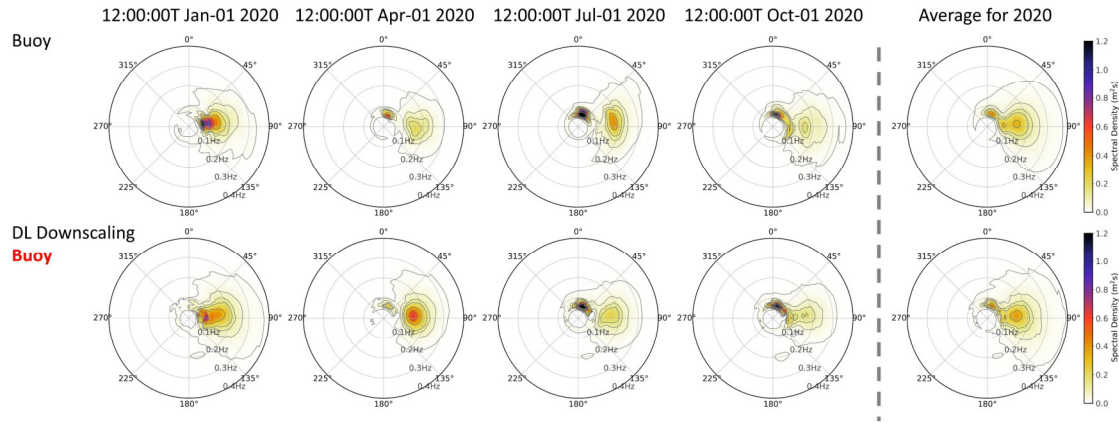


Figure S11. The comparison of directional wave spectra (DWSs) between the results from buoy reconstruction and from Deep Learning (DL) downscaling using buoy data as training targets. The 1st row is the corresponding buoy reconstructed DWSs, and the 2nd row is the results from the DL downscaling model using buoy DWSs as the training target. The four columns to the left of the dashed line in each row are the corresponding DWSs at four arbitrarily selected time points. The two DWSs to the right of the dashed line in each row are the corresponding annual mean DWSs in 2020.

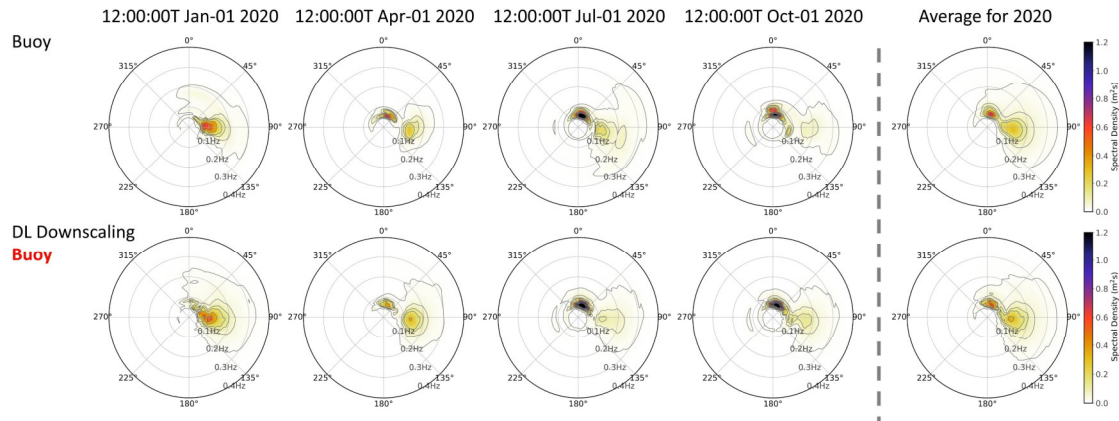


Figure S12. The same as Figure S11, but for buoy CDIP045.

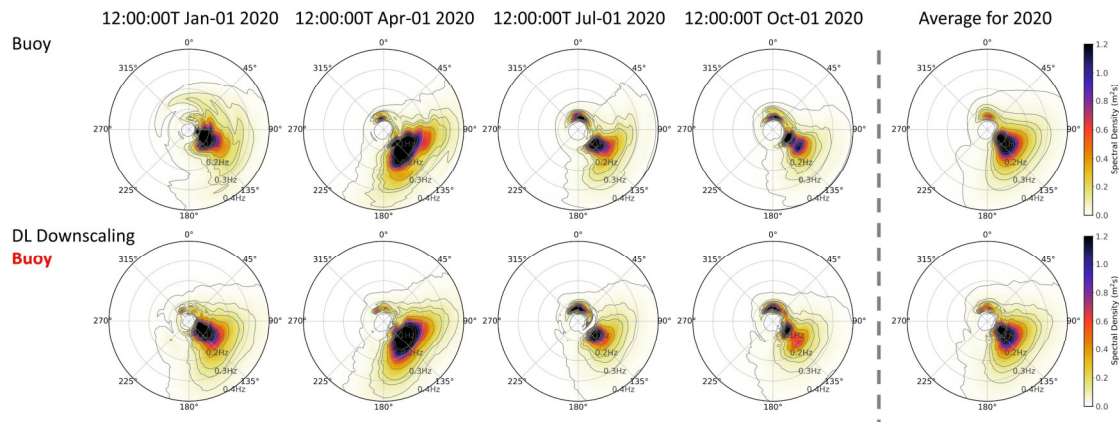


Figure S13. The same as Figure S11, but for buoy CDIP067.

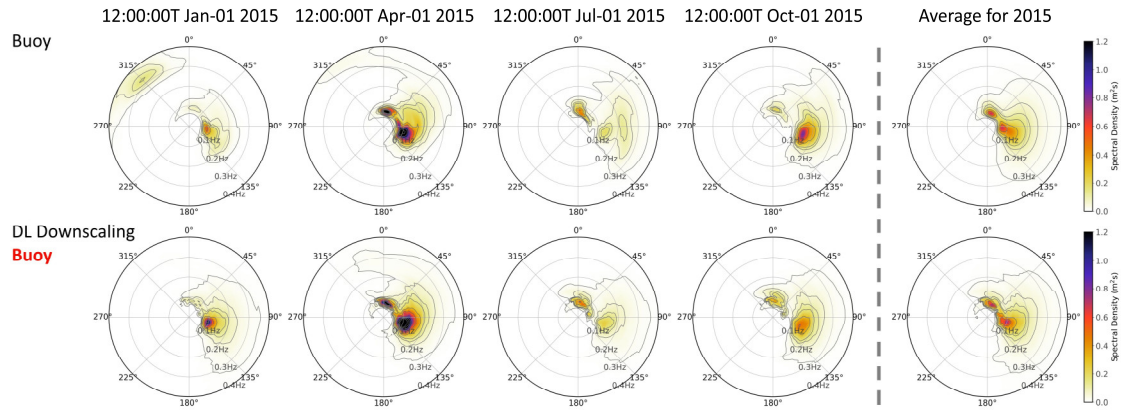


Figure S14. The same as Figure S11, but for buoy CDIP093. Because CDIP093 does not have the data for year 2020, the data of 2015 is used instead (the data is not used in the training process)

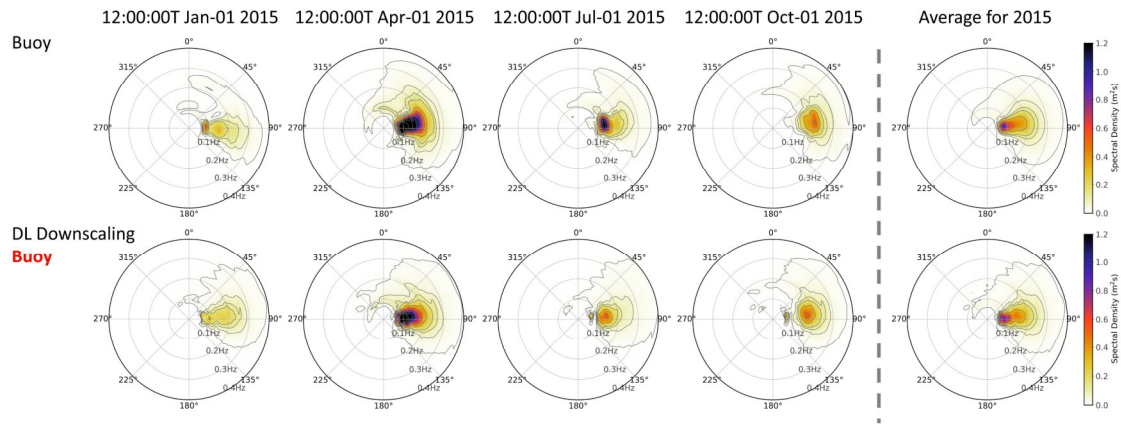


Figure S15. The same as Figure S11, but for buoy CDIP107. Because CDIP107 does not have the data for year 2020, the data of 2015 is used instead (the data is not used in the training process).